

Learning Multimodal Affinities for Textual Editing in Images

OR PEREL, Amazon Web Services
 ORON ANSHEL, Amazon Web Services
 OMRI BEN-ELIEZER, Harvard University[†]
 SHAI MAZOR, Amazon Web Services
 HADAR AVERBUCH-ELOR, Cornell-Tech, Cornell University[†]

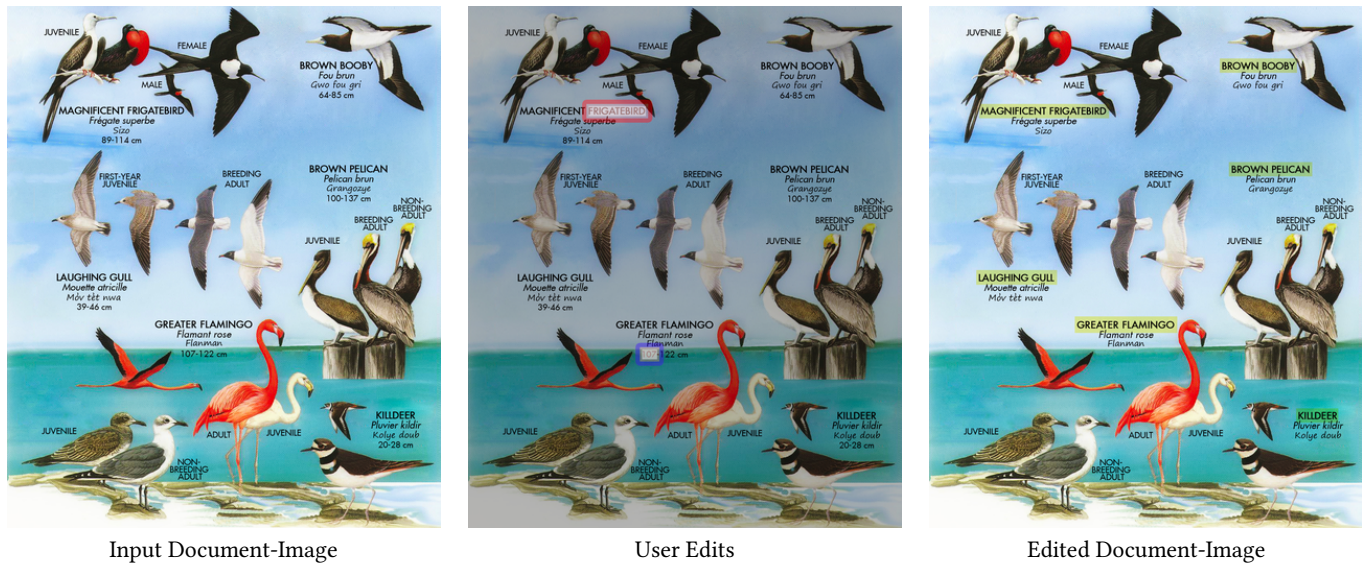


Fig. 1. Given a document-image (left), we learn multimodal affinities among the textual entities. The user can then select words to edit. For example, the user can select to highlight the word “FRIGATEBIRD” marked in red or delete the word “107” marked in blue (center). Our method propagates the editing operations onto words that are semantically and visually similar, highlighting all bird names and removing their size information (right). Image courtesy: Société Audubon Haiti.

Nowadays, as cameras are rapidly adopted in our daily routine, images of documents are becoming both abundant and prevalent. Unlike natural images that capture physical objects, document-images contain a significant amount of text with critical semantics and complicated layouts. In this work, we devise a generic unsupervised technique to learn multimodal affinities between textual entities in a document-image, considering their visual style, the content of their underlying text and their geometric context within the image. We then use these learned affinities to automatically cluster the textual entities in the image into different semantic groups. The core of our approach is a deep optimization scheme dedicated for an image provided by the user that detects and leverages reliable pairwise connections in the multimodal representation of the textual elements in order to properly learn the affinities. We show that our technique can operate on highly varying images spanning a wide range of documents and demonstrate its applicability

Authors’ addresses: Or Perel, Amazon Web Services, orperel@amazon.com; Oron Anshel, Amazon Web Services, oronans@amazon.com; Omri Ben-Eliezer, Harvard University[†], omribene@cmsa.fas.harvard.edu; Shai Mazor, Amazon Web Services, smazor@amazon.com; Hadar Averbuch-Elor, Cornell-Tech, Cornell University[†], hadarelor@cornell.edu.

© 2021 Association for Computing Machinery.
 This is the author’s version of the work. It is posted here for your personal use. Not for redistribution. The definitive Version of Record was published in *ACM Transactions on Graphics*, <https://doi.org/10.1145/3451340>.

for various editing operations manipulating the content, appearance and geometry of the image.

CCS Concepts: • **Computing methodologies** → **Unsupervised learning; Neural networks; Learning latent representations; Instance-based learning; Image manipulation;**

Additional Key Words and Phrases: image editing, multimodal representations, vision and language, clustering, document images, infographics

ACM Reference Format:

Or Perel, Oron Anshel, Omri Ben-Eliezer, Shai Mazor, and Hadar Averbuch-Elor. 2021. Learning Multimodal Affinities for Textual Editing in Images. *ACM Trans. Graph.* 1, 1, Article 1 (January 2021), 16 pages. <https://doi.org/10.1145/3451340>

1 INTRODUCTION

We, as humans, commonly view natural images as those that contain physical objects, such as people, cars or flowers. However, a significant portion of the images uploaded to the internet capture documents. This calls for automated generic methods to understand, organize and manipulate text in images, and specifically in

[†] Work done while Omri Ben-Eliezer and Hadar Averbuch-Elor were with Amazon Web Services.

document-images. A fundamental ability useful for this type of tasks is the automatic *clustering* of text in images, where each cluster corresponds to a unique “category” of words, similar in meaning and context within the document. For example, for the infographic depicted in Figure 1, possible text categories could be species names, Latin names, species size, gender, or age (juvenile vs. adult).

Documents come in large variety. However, while there are countless datasets of images capturing groundable objects which include various granularities such as per-pixel segmentation maps, datasets of document-images are sparse and semantically labeling new documents is prohibitively expensive. Therefore, in this work, we propose a generic unsupervised method to learn meaningful affinities among textual elements in document-images, allowing to cluster them into (implicit) categories, whose number is not given in advance. Our method processes the image in several steps. First, it obtains text entities from the image using an off-the-shelf OCR technique, and extracts several types of high-dimensional features which represent the *visual* style of these entities, *geometric* context within the document, and *semantic* content of the underlying words. As it turns out, clustering in this high-dimensional feature space does not yield good results, as the affinities among textual elements are noisy and some of the semantic groups are intermixed. As we show, this also holds true for features originating from a single modality (see, e.g., the style-based features visualized in Figure 2).

Thus, we devise a constraint-based optimization scheme, which generates a low-dimensional representation for the words in the document, especially suitable for clustering purposes (see Figure 3). This optimization scheme is our main technical contribution; for each image provided by the user, it leverages reliable pairwise connections extracted automatically from the initial representation of the textual entities and optimizes the learned affinities. During training, the latent representations of pairs that constitute “must-link” constraints are drawn closer together, while “cannot-link” pairs are pushed towards far-away parts of the latent space. With the learned affinity, one can group close-by entities in the latent space. Furthermore, if needed, our pair-based approach enables augmenting the information with labeled pairs to constitute a semi-supervised framework, allowing the user to refine the affinity space with several user-drawn scribbles that describe pairs of words that should or should not be grouped together.

The ability to learn meaningful textual affinities in images can have a multitude of applications, such as document editing, similarity analysis, or locality sensitive hashing of document-images. To practically demonstrate one useful application of our framework, we show how the cluster-based representation can very easily accelerate text editing tasks in images, even when one does not have access to the source code of the document (for example, when a graphic designer wishes to generate a slightly modified version of a text layout found on the web).

Editing textual content in document-images can be a tedious task, especially if the amount of text entities is large, as the editing operations are repetitive in many cases. Some examples of such potentially repetitive tasks include changing the font type, size, or color for all content of a given type, updating all occurrences of date and time in a schedule sheet, aligning the names of all dishes in a menu to be in the same column, or removing content of a certain

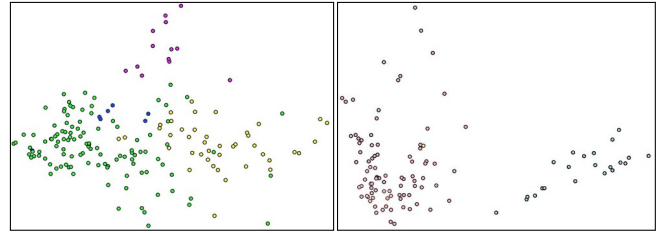


Fig. 2. Style-based affinity space *without* our optimization scheme. Above we visualize the affinity space obtained from style-based features only on the examples illustrated in Figures 3 (left above) and 4 (right above). The points are colored according to the clustering provided in the corresponding figures. As the figure illustrates, even for features originating from a single modality (style-based in this case), the initial affinities are noisy and thus challenging to cluster.

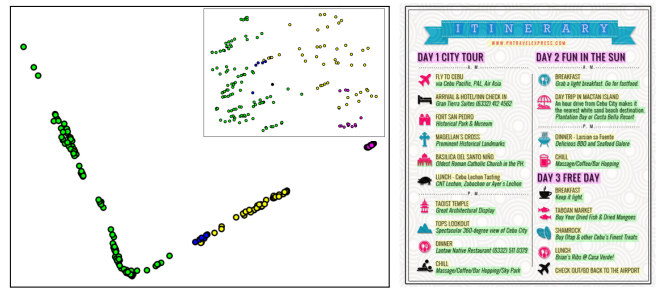


Fig. 3. Above we use PCA to visualize our affinity space before and after our optimization scheme (left). The projected points are colored according to the output grouping result (right). As the figure illustrates, before the optimization stage some of the semantic groups are intermixed and would not allow for measuring high-quality affinities (left image, top-right corner). After the optimization, the affinities are significantly more tightly clustered. Original image © PH Travel Express.

type (see Figure 1). Efficiently propagating a sparse set of user edits in an image has received considerable attention in the context of color and tonal editing [Chen et al. 2012; Farbman et al. 2010; Li et al. 2008]. Typically, editing operations are propagated to pixels of similar appearance, bypassing the need to perform a careful region selection and matting. In our setting, we propagate textual edits in the document-image by simply applying an edit performed on a single text entity to its whole cluster.

We supplement our clustering and edit propagation approach for document-images with a new publicly available dataset of 50 document-images spanning multiple types of infographics, including menus, schedules, brochures, and maps, as well as dense documents which we quantitatively evaluate our approach on.

Explicitly stated, our main contributions are:

- A constraint-based optimization scheme for learning affinities among words in document-images, taking into account multimodal features of the words.
- A generic unsupervised approach to group textual elements in documents by similarity, without the need to define semantic

categories (e.g. title, paragraph, caption) in advance, useful for textual editing in images.

- A new dataset of document-images of various types, useful as a baseline for future works on document-image analysis.

2 RELATED WORK

In what follows, we elaborate on the most closely related work.

2.1 Textual Analysis in Images

Automated structural analysis of document-images has been of interest for more than thirty years [Kasturi et al. 2002]. Earlier works relied on predetermined logical rules and heuristics to solve either high level global tasks such as layout and hierarchy analysis, and skew detection, or local tasks such as high-accuracy OCR detection; see e.g. [Akiyama and Hagita 1990; O’Gorman 1993] and the references within, as well as the comprehensive book of Baird et al. [1992]. However, due to their reliance on heuristics with which it is hard to capture all possible end-cases, these classical approaches typically experience difficulties when performing global analysis of documents with complex layouts. Breuel [2002; 2003] proposes efficient and exact geometric algorithms for some tasks typically arising in document layout analysis, thus overcoming the need for heuristics in these tasks.

Recent works have used neural networks to conduct global analysis of document images in a more robust and nuanced manner. Most notably, Yang et al. [2017] follow a multimodal approach to extract the semantic structure from document images. The structure extraction is viewed as a pixel-wise segmentation task – i.e., as the task of segmenting the pixels of the document image into several type of predefined labels, with examples such as “paragraph”, “list”, and “section heading”. To train their network, they devise a suitable synthetic document generation process. Their work shows that joint textual and visual embeddings of pixels in a document image aids in segmentation tasks. While our work also uses a multimodal embedding for the textual elements in the image, it significantly diverges from [Yang et al. 2017] in that it is unsupervised, and performs grouping without the need for pre-defined labels, allowing to flexibly group the words in the document into an unknown number of clusters, whose characteristics are not known in advance.

Many of the examples of documents we consider in this paper are *infographics*; these are documents which present information or data visually, in a way that is effective and easy to digest for the reader. Unlike dense documents, which typically admit a more standard and unified structure, infographics come in a variety of visual structures and automatically extracting information from them requires specialized machinery. There has been a multitude of works on parsing and understanding infographics. Kembhavi et al. [2016] propose Diagram Parse Graphs, a novel logical representation for diagrams, and use them for question-answering on diagrams; Bylinskii et al. [2017; 2018] extract predictive visual information from infographics by studying connections between the textual and the visual elements; Poco and Heer [2017] automatically parse and analyze visual encodings in charts and graphs; Chen et al. [2020] devise a deep learning based approach for designing

timeline infographics. Lu et al. [2020] analyze infographics following the Visual Information Flow, the implicit semantic structure in which graphic elements are organized so as to convey information to the reader. Common to all of these works is that they analyze the role of textual elements in infographics as part of the general visual structure. However, none of them directly addresses the task of clustering “similar” text entities, discussed in this paper.

Other previously investigated tasks that were shown to benefit from a joint visual and textual representation include, e.g., visual question answering [Agrawal et al. 2018; Antol et al. 2015; Goyal et al. 2018] and image captioning [Donahue et al. 2017; Karpathy and Fei-Fei 2017]. Detection and understanding of text in the wild – recognizing text in natural scene images – has also been thoroughly investigated, see e.g. [Jaderberg et al. 2016].

2.2 Image Editing and Edit Propagation

Image editing is a central application in computer graphics and has significantly advanced over the past several decades. One of the first works in automatic image editing [Pérez et al. 2003] presents a method to seamlessly edit regions in images, based on Poisson equations. Patch-based approaches have also shown to be useful throughout the years (e.g., [Barnes et al. 2009]). In recent years, most of the computer graphics image editing techniques have been based on deep neural networks. Specifically, various works have shown that training generative models using a GAN framework [Goodfellow et al. 2014] is effective for image generation and manipulation. As an example, [Liu et al. 2018] recently achieved remarkable results for image completion.

Our work adds to the long line of works that develop automated editing procedures aiming at reducing human effort within the editing process. Specifically, there have been various works on propagating visual image editing. For example, Li et al. [2008] show that the combination of edge-aware interpolations with a classification step is effective for speeding up editing of image regions via user scribbles. An and Pellacini [2008] show that edit propagation can be viewed as a linear problem, where a sparse set of user edits combined with structural observations on the underlying linear system suffice to robustly propagate edits between different entities. Xu et al. [2009] show that adaptive clustering with the help of k -d trees can significantly speed up the approach of [An and Pellacini 2008] without affecting the visual quality of the resulting edits. Farbman et al. [2010] observe that, for the sake of evaluating the similarity between pixels for editing purposes, it is helpful to replace the usual Euclidean distance between pixels with so-called diffusion distances. Chen et al. [2012] consider a different approach for edit propagation, which seeks to maintain the topology of the image through preservation of its manifold structure. Xing et al. [2014] devise a system that automatically completes repeated patterns while painting, allowing the user to avoid repetitive drawing tasks. Finally, a recent work of Meyer et al. [2018] presents an intriguing deep learning framework to propagate color changes along videos, combining local and global approaches to ensure the stability and consistency of the solution.

2.3 Document Editing

While we mainly target document-images and are only provided with an image of a document, our approach can also be used to analyze documents in their raw format. Commercial software products for creating and managing documents with highly complex layouts include, e.g., Adobe InDesign¹ and FrameMaker², and Microsoft Publisher³, among many others. [Saund et al. 2003] propose a content-aware toolkit to perform various editing operations on documents, relying on local grouping of the text elements. To this end, Project Naptha⁴ is a popular OCR-based Google Chrome extension allowing the user to perform multiple basic editing operations in web-pages, including copying, highlighting, editing and translation of text. While the above systems and works provide numerous sophisticated tools for high-quality editing of documents with complex layouts, we are not aware of any product and/or previous work that allows automatic global similarity analysis and grouping as is done in our work. Incorporating our global similarity analysis capabilities into existing solutions for document analysis might serve as an interesting venue for future research, making these solutions more similar to the way humans perceive documents.

2.4 Affinities and Clustering in Images

Our approach aims to learn an affinity, i.e., a measure of similarity, between (textual) objects in (document-)images. Analysis of similarity in images has been a widely studied task. For example, [Garces et al. 2014] devise a style-based similarity measure for objects in clip art images, relying only on visual features (and not on content): specifically, on color, shading, texture, and stroke features.

At the core of our approach is a deep optimization scheme for clustering textual data into an unknown number of clusters. Data clustering is one of the most fundamental problems in data analysis, highly applicable to different fields of science, and is especially essential in an unsupervised learning scenario. Traditionally, clustering techniques focused on the grouping task and assumed a representation is provided as input. However, recently, clustering methods have coupled the feature learning and the grouping stages into one unified deep optimization scheme. Xie et al. [2016] use a stacked autoencoder to learn a deep representation which is easier to group onto a known number of cluster centroids. Later works (e.g., [Dizaji et al. 2017; Yang et al. 2016]) have been able to boost performance for images using convolutional networks. More closely related to our work, Shah and Koltun [2018] and Fogel et al. [2018] use pairwise constraints to learn a cluster-friendly representation without prior knowledge on the number of clusters in the data. These works operate on the images directly, leveraging a reconstruction loss to learn an initial embedding space. In our work, we are interested in learning semantic affinities between words in the image and thus initialize the latent space using multimodal features that encode both the style and the content of the extracted words.

¹<https://www.adobe.com/products/indesign.html>

²<https://www.adobe.com/products/frame-maker.html>

³<https://products.office.com/en-us/publisher>

⁴<https://projectnaptha.com/>

3 OVERVIEW

In this work, we consider the problem of learning affinities for clustering textual elements in an image, and demonstrate the use of this clustering primitive for edit propagation purposes. Our underlying assumption is that we do not have access to any meta-data on the analyzed document, and so our learned affinities and resulting clustering are based purely on the information extracted from the image of the document. The existence of such meta-data, however, would significantly ease the clustering task as it would provide additional constraints which can be leveraged for learning the textual affinities.

Our solution first extracts multimodal features for any textual element in the image; then, it learns a suitable notion of affinity for the elements within the document in an unsupervised manner; and finally, the affinity notion is leveraged to cluster words into the desired groups. In more detail, our solution constitutes of the following steps.

Identifying basic elements. The main challenge in our context is the understanding of text semantics. Thus, while the basic elements in previous works have usually been pixels, here we use words as the basic elements. As OCR-related works have essentially solved the challenge of word-level identification, we first use an off-the-shelf OCR method to extract words and other symbols in the image, and use these as our basic textual elements. Then, as basic elements located very close to each other tend to be semantically related, we group our basic elements into *contextual-lines* (see Section 4).

Extracting multimodal features. To be able to devise an affinity measure for the basic elements in our context, we need a suitable representation that will capture their “essence”. The representation, described in detail in Section 5, captures multimodal features of the textual elements, which can be divided into three families:

- Style-based features, which refer to the visual appearance of words. Using a pre-trained classifier, we extract visual features related to font characteristics for each word.
- Content-based features of words capturing the semantic meaning of the word in a broader context, considering its enclosing contextual-line.
- Geometric features, concerned with the size and location of the words within the document.

Constraint-based affinity learning. Our next main challenge is to learn an affinity measure for our multimodal space.

Pairwise constraints. As our approach is unsupervised, to guide the learning we extract *pairwise constraints*, which are reliable pairwise connections between words in the document. We derive several types of pairwise connections in two categories: *must-link* constraints that correspond to pairs that are very similar according to our analysis (the training process will pull such pairs towards each other in the affinity space), and *cannot-link* constraints, corresponding to pairs of “very different” words that should be far apart in the affinity space (see Section 6.1).

Affinity Space Optimization. Our objective now is to learn an affinity measure. Formally, suppose that the multimodal representations obtained above are given as D -dimensional vectors. We consider

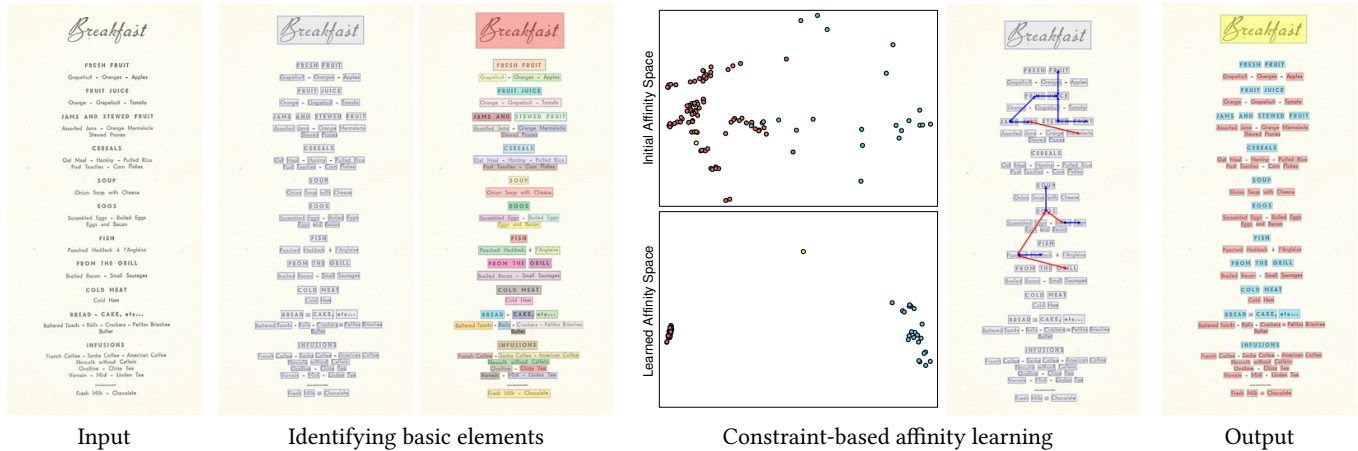


Fig. 4. Given a document-image (left), we first extract words and contextual-lines within the image. To initialize the latent affinity space, we extract multimodal features for each word in the image. We then learn the semantic affinities among words in the image by leveraging reliable pairwise connections in the form of must-link (marked with blue arrows) and cannot-link (marked with red arrows) constraints. Finally, we use the learned affinities to obtain semantic groups for edit propagation tasks (right). Image courtesy: Compagnie générale transatlantique.

a low-dimensional latent space \mathbb{R}^d coupled with an affinity measure σ for vectors in \mathbb{R}^d , which outputs 1 for “similar” vectors and close-to-0 values for “very different” vectors. In practice, $d \ll D$. Our objective is to train a network $f_\theta: \mathbb{R}^D \rightarrow \mathbb{R}^d$ with the goal of having $\sigma(f_\theta(Z_i), f_\theta(Z_j)) \approx 1$ (high affinity value) for pairs of similar words with representations Z_i, Z_j , and a much smaller affinity value when Z_i and Z_j are not similar. For training, we use a Siamese architecture, feeding pairs of must-link/cannot-link words to two identical copies of the network along the training process; roughly speaking, the loss we aim to minimize during training “punishes” us for must-link constraint pairs Z_i, Z_j with $\sigma(f_\theta(Z_i), f_\theta(Z_j)) \ll 1$ and for cannot-link pairs when $\sigma(f_\theta(Z_i), f_\theta(Z_j)) \approx 1$. See Section 6.2 for more details (and Section 9 for further implementation details).

Clustering in affinity space. Finally, we use our now trained network f_θ and the learned affinities in order to obtain the desired groups for edit propagation (see Section 7).

4 BASIC TEXTUAL AND CONTEXTUAL ELEMENTS

We first extract the basic textual elements in the input image. To do so, we use standard techniques to detect word bounding boxes and recognize the words within these bounding boxes [Smith 2007]. Isolated words are not sufficient to effectively analyze natural language. Thus, we augment our basic textual elements with a contextual notion by grouping close-by words and associating a *contextual-line* to each extracted word.

We follow classical approaches in the literature (see e.g. [Baird et al. 1992]) and pick the contextual-lines as the connected components of a suitable sparse graph representation of the document-image. We obtain contextual-lines by grouping horizontally adjacent words that contain similar geometric attributes. Specifically, we construct an edge-weighted graph of word boxes, where the weight between a pair of words is the horizontal space-to-height ratio between them, normalized by the aspect ratio (image width divided by image height). Formally, given two word bounding boxes B_i and

B_j whose y -coordinates have a sufficiently large overlap, denote the heights of the boxes B_i, B_j by h_i, h_j respectively, the horizontal space between them by s , and the aspect ratio of the image by r . We then define the weight of the corresponding edge by

$$w(B_i, B_j) = \frac{s \cdot r}{\max(h_i, h_j)}.$$

We then define a sparse graph representation by removing edges whose weights are above a predefined threshold (empirically set to 0.1). The connected components in this sparse graph form our contextual-lines.

It should be noted that we deliberately avoid more sophisticated approaches to extract lines and paragraphs (e.g., [Bruehl 2002, 2003]). Indeed, we seek to group words into contextual-lines as conservatively as possible, so as to avoid grouping words with different contexts into the same contextual-line at all costs. We then use a neural network, described in the next sections, to learn the non-local affinities.

5 AFFINITY SPACE INITIALIZATION

As described in the previous section, the basic textual element we consider is a word unit, henceforth denoted by U_w , which can be described visually by its associated image region or semantically by its underlying content. To augment words with a contextual notion, each word is associated with a contextual-line, henceforth denoted by U_l . We initialize our affinity space by extracting multimodal features for each word in the image and concatenating them to obtain our aggregated word representation $Z(U_w, U_l)$. Explicitly stated, our initial representation Z is defined as

$$Z(U_w, U_l) = [\mathbf{f}_s(U_w), \mathbf{f}_c(U_w, U_l), \mathbf{f}_g(U_w)],$$

where $\mathbf{f}_s(U_w)$ encodes the visual style, $\mathbf{f}_c(U_w, U_l)$ encodes the semantic content and $\mathbf{f}_g(U_w)$ encodes geometric attributes. Next, we describe these multimodal encoders in more detail.



Fig. 5. Training samples used for training a style encoder. In each row, we randomly select samples belonging to the same class. As illustrated above, the classes vary in font characteristics, including font-family, font-weight and style.

5.1 Style Encoder

The style encoder $\mathbf{f}_s(U_w)$ aims to extract the visual appearance of a word U_w . In our setting, visual appearance can roughly be estimated using font characteristics. Therefore, we pre-train a classifier to distinguish between multiple font characteristics such as font-family, font-weight (regular/bold) and style (regular/italics). Specifically, we employ a Residual Network (ResNet) architecture [He et al. 2016] as a visual feature extractor trained on a synthetic dataset we generate using an open source synthetic data generator⁵.

Figure 5 illustrates samples belonging to three different classes (out of the 138 classes used during training). As illustrated in the figure, a unique configuration of font-family, font-weight and style is determined for each class. The content, background, color, and font-size vary for each sample, to encourage invariance to these properties. Note that while the text color could be considered part of its *style*, we noticed that in many cases the color may vary (even within the same contextual element), making it an unreliable cue.

At test-time we use the last layer of the trained classifier (that is, the input to the last fully connected layer in the ResNet architecture) as a visual feature representation for each basic unit in the document-image.

5.2 Content Encoder

The content encoder $\mathbf{f}_c(U_w, U_l)$, captures semantic language features of a word U_w . Contextualized language-model encoders are recently gaining increasing popularity, as they capture the semantic meaning of the word in a broader context, considering its enclosing phrase. Thus, we employ a contextualized language-model encoder which operates on a word U_w and its enclosing contextual-line U_l , thereby capturing the word meaning in the context of that phrase.

In our work, the content encoder $\mathbf{f}_c(U_w, U_l)$ is a concatenation of the state-of-the-art forward and backward models detailed in Akbik et al. [2018]. The implementation we used was pre-trained on a large corpora of unlabeled data, and no additional tuning was

⁵<https://github.com/Belval/TextRecognitionDataGenerator>

performed. Please refer to [Akbik et al. 2018] for further details on the model architecture and training.

5.3 Geometry Encoder

Lastly, as document entities tend to follow aligned patterns, we employ a simple descriptor to capture geometric attributes. Specifically, for each word U_w with associated image coordinates (normalized to $[0, 1]$), the geometry encoder $\mathbf{f}_g(U_w)$ is defined as follows:

$$\mathbf{f}_g(U_w) = [x, y, w, h], \quad (1)$$

where (x, y) is the top-left corner of the bounding box of U , and w and h are the width and height of the bounding box, respectively.

6 CONSTRAINT-BASED LEARNING OF AFFINITIES

Our approach crucially relies on *learning* an appropriate *affinity* measure between the multimodal representations of words in the document. In this section we describe how to learn such a measure. The goal is that pairs of words with high similarity in terms of style, content, and geometry will be close by according to the learned affinity, whereas pairs of words that are not similar will be far apart in this affinity space.

Our setting is unsupervised; to learn a suitable affinity measure, we must be able to automatically generate constraints, which will then serve as a basis for the learning process. To this end, we generate two types of pairwise constraints (i.e., constraints between pairs of words) in which we are relatively confident: *must-link* constraints, indicating that a pair of words are highly similar, and should have a small distance between them; and *cannot-link* constraints, for pairs of words that are “very different”, implying that the distance between them should be high. The constraints are described in-depth below, in Subsection 6.1; see Figure 6 for a visualization. They are then fed to a Siamese network, which outputs an affinity measure (a real number between zero and one) given any pair of word units, see Subsection 6.2.

6.1 Generating Pairwise Constraints

We employ three different types of constraints: intra-contextual *must-link* constraints of words that reside within the same contextual-line, inter-contextual *must-link* constraints and inter-contextual *cannot-link* constraints. To generate inter-contextual constraints, we examine high-confidence pairs using a set of rules combining the different modalities and consolidate the results over the multiple domains (i.e. by taking constraints which do not violate any of the modalities). Finally, we balance the set of constraints by downsampling the constraints such that *must-link* constraints constitute 60% of the total number of constraints. Next, we describe our intra- and inter- contextual constraints.

Intra-Contextual Constraints. In Section 4, we defined the concept of a contextual-line as a basic unit that captures the context of a word. We conservatively grouped only horizontally close-by words with similar geometric properties. Thus, to encourage words within the same contextual-line to output a similar representation, we define intra-contextual *must-link* constraints, which connect pairs of words belonging to the same contextual-line.



Must-link Constraints

Cannot-link Constraints

Fig. 6. Generating intra- and inter-contextual constraints. Above we illustrate the various constraint types in our framework. Left: We consider must-link constraints between words which either share the same context (marked with light blue arrows) or are highly similar in terms of all the criteria detailed in Section 6.1 (marked with pink arrows). Right: Cannot-link constraints are defined between pairs of words that are different according to visual-style (marked with a yellow arrow), language-syntax (marked with a green arrow), language-semantics (marked with a red arrow) or geometry (marked with a blue arrow). Original image © Demco, Inc.

Inter-Contextual Constraints. In addition to the local intra-contextual must-link constraints, we would like to encourage high affinity pairs, which are not necessarily spatially close, to be pulled closer together. Likewise, to avoid the trivial solution that would collapse all words to a single point, we would like to encourage words that are clearly different to be pushed further apart.

Following the human understanding of what is perceived as close on a document, we define a set of rules spanning the multiple modalities we consider. Inter-contextual *must-link* constraints are defined conservatively between pairs of words which are considered similar in all aspects. In contrast, inter-contextual *cannot-link* constraints are defined between pairs of words that are different in at least one aspect, as a significant difference in even one criterion suggests that these words should not be close in the learned affinity space. To this end, we consider the following criteria:

Visual-style similarity. To extract pairs that are highly similar (or different) in style, we extract pairwise similarities between all visual feature representations, which are described in Section 5.1. Pairs of points are considered visually-close if they are connected to a mutual-kNN graph. In other words, two points are visually-close only if they are both among each other's k -nearest neighbors. Likewise, pairs of points are considered visually-different if they are mutually-far. In both cases, we empirically set $k = 6$.

Language-syntax criterion. Words are sorted into three bins according to the types of characters that compose them: entirely uppercase, entirely lowercase, and mixed. Words belonging to the same bin are considered similar in syntax and words belonging to different bins are considered different in syntax.

Language-semantics criterion. Named-entity recognition (NER) is a common task in language processing. In this task, words representing semantic entities may be tagged according to some predefined categories such as ordinals, percentages, time-expressions, person-names, organizations, and so on. To encourage semantically based constraints, we employ a NER tagger over word tokens per contextual line. Then, we carefully look at the tagged words and characterize their respective contextual lines, that is, according to the named entities contained within them. Contextual lines defined by multiple types of named entities are considered semantically "noisy" and therefore their words do not yield constraints. Instead, we generate constraints only for words that characterize their associated contextual-line. Standalone words which are tagged similarly are considered similar in semantics, while standalone words that are tagged differently are considered different in semantics. We use the NER implementation provided by Akbik et al. [2018].

Geometric considerations. We use the bounding-box height dimension to deduce whether two words are similar or not in terms of geometry. Denote the respective bounding-box heights as h_1 and h_2 . Assuming $h_1 > h_2$, we consider the bounding-box height ratio h_1/h_2 . If the ratio is below a predetermined threshold (1.25 in our implementation), the words are considered similar in terms of size. Otherwise, they are considered different.

6.2 Affinity Space Optimization

Next, we wish to use the constraints to learn a continuous affinity measure for words. We solve an optimization problem over *soft* (possibly contradicting) constraints by employing a Siamese network, that learns a suitable *embedding* of the words into a latent

low-dimensional affinity space; See, for example, the visualized affinity space in Figure 3. The value outputted by the network given a pair of words will then serve as our affinity measure between these words.

Formally, let $\{U_w^1, \dots, U_w^N\}$ denote the word units in the document-image, and for each word U_w^i , let Z_i denote its aggregated representation as defined in Section 5. We view these representations as D -dimensional real vectors, i.e., $Z_i \in \mathbb{R}^D$, where the dimensionality D is determined by the aggregated representations. The latent low-dimensional affinity space is defined as (\mathbb{R}^d, σ) , i.e., its dimensionality is set to d . The value of d is chosen to address the following two issues: On one hand, it should be low enough to avoid the inherent complexities of clustering in high dimensions as much as possible (the so-called ‘‘curse of dimensionality’’). On the other hand, recall that our end-goal is to perform a clustering on the latent affinity space, so that each cluster represents a group of similar elements. Conceptually speaking, each pair of clusters might have a different semantic ‘‘reason’’ as to why these clusters are different from each other. Thus, to be able to separate each pair of clusters in the latent affinity space, it makes sense that this space will have roughly one coordinate for each pair of clusters. Therefore, to properly handle document-images where the number of clusters is k , our latent dimensionality should be at least $d \approx \binom{k}{2}$.

The affinity function $\sigma: \mathbb{R}^d \times \mathbb{R}^d \rightarrow [0, 1]$ is defined, given $\mathbf{u}, \mathbf{u}' \in \mathbb{R}^d$, by

$$\sigma(\mathbf{u}, \mathbf{u}') = \exp(-\|\mathbf{u} - \mathbf{u}'\|_2^2), \quad (2)$$

approximating the similarity function suggested by [Fathi et al. 2017]. To this end, a larger affinity value between a pair of words corresponds to ‘‘higher similarity’’ between these words.

Our objective is now to optimize the parameters of a network $f_\theta: \mathbb{R}^D \rightarrow \mathbb{R}^d$, so that given two word units U_w^i and U_w^j whose corresponding representations are Z_i and Z_j , the affinity between the embeddings, which equals

$$\sigma(f_\theta(Z_i), f_\theta(Z_j)), \quad (3)$$

would be a good estimate for the actual similarity between these two words. We use a Siamese architecture to train the network (see Section 9 for implementation details). We pick pairs of words Z_i, Z_j satisfying one of the constraints defined in the previous subsection, and feed them to two identical copies of the network. We use the function σ for its probabilistic interpretation, as $\sigma(f_\theta(Z_i), f_\theta(Z_j))$ in a sense predicts the likelihood that the two points (U_w^i, U_w^j) belong to the same ‘‘category’’ in the data. For a pair of points whose embeddings $f_\theta(Z_i), f_\theta(Z_j)$ are almost identical, we have $\sigma(f_\theta(Z_i), f_\theta(Z_j)) \approx 1$. On the other hand, when the embeddings are entirely different, $\sigma(f_\theta(Z_i), f_\theta(Z_j)) \approx 0$. This function is also numerically stable for training using a cross-entropy classification loss. Explicitly stated, we train our Siamese network to minimize the following loss:

$$L = - \sum_{(i,j) \in E_{\text{must-link}}} \log(\sigma(f_\theta(Z_i), f_\theta(Z_j))) \\ - \sum_{(i,j) \in E_{\text{cannot-link}}} \log(1 - \sigma(f_\theta(Z_i), f_\theta(Z_j))),$$

where $E_{\text{must-link}}$ is the set of all pairs (i, j) for which a must-link constraint was added for the pair (U_w^i, U_w^j) , and $E_{\text{cannot-link}}$ is defined similarly with respect to cannot-link constraints.

7 AFFINITY SPACE CLUSTERING

In order to demonstrate how the learned affinities can be used, in this work we are interested in propagating textual edits. Edit propagation frameworks typically aim at propagating color and tonal edits according to the user scribbles. Thus, previous works use the affinities between pairs of pixels to output the blending weights associated with the different user edits. Unlike the continuous color and tonal edits, in our setting, we seek a binary decision per word. For each word the user selects to edit, we propagate the edit onto all the words that are highly ‘‘similar’’ to it, where similarity can be measured in the affinity space described in previous sections.

Thus, we wish to group the words into several clusters of highly similar elements; this would allow us to simultaneously perform editing operations on all words in a given cluster. To obtain such clusters, we group the contextual-lines according to a mean likelihood estimate that the words within these contextual-lines should be grouped together, where the likelihood estimate corresponds to the notion of affinity obtained in the previous section. Explicitly stated, for a pair of contextual-lines U_l and U_l' , we compute the likelihood that U_l and U_l' belong in the same cluster in the data by leveraging a voting mechanism. Specifically, consider the trained network $f_\theta: \mathbb{R}^D \rightarrow \mathbb{R}^d$ and the affinity function σ defined in Equation (2). Given each pair of word units (U_w^i, U_w^j) with multimodal representations Z_i, Z_j , where U_w^i belongs to U_l and U_w^j belongs to U_l' , we estimate the affinity of Z_i and Z_j using Equation (3), and then average all such estimates to obtain a likelihood that the two contextual-lines U_l and U_l' should be grouped together.

We then construct an edge-weighted graph of contextual-lines, where the edge connecting a pair of contextual-lines is weighted according to the likelihood estimates. The graph is further pruned by disregarding edges between incompatible contextual-lines (whose bounding box heights are above a constant ratio of 1.25) and whose weights correspond to a likelihood below a predetermined threshold of 0.75. The words within the connected components of our contextual-lines graph form our final clusters.

8 EXTENSION TO AN INTERACTIVE FRAMEWORK

Our optimization scheme can naturally be extended to an interactive framework, allowing one to incorporate user inputs in order to refine the affinity space, if needed. To do so, we first run our algorithm offline, and proceed to augment our automatically obtained pairwise constraints with user-supplied ones.

Our interactive tool supports a lasso selection tool. In the case of must-link constraints, pairwise constraints are generated among all words in the selection group. For cannot-link constraints, we offer a similar mechanism requiring two clicks for selecting the disjoint groups. We follow up with cannot-link constraints between all pairwise elements from both groups. We keep all pairwise constraints and do not sub-sample the user constraints. Furthermore, we remove automatically-generated constraints which violate the

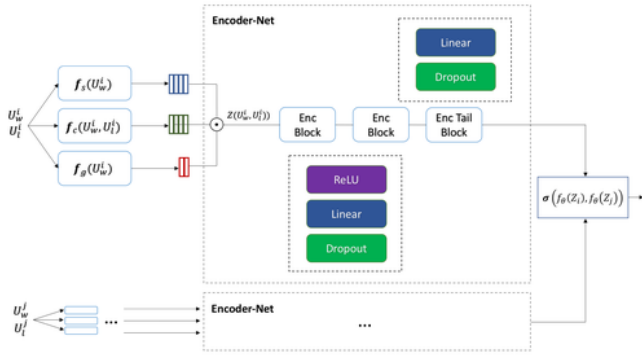


Fig. 7. Siamese encoder network architecture. The input of the pipeline is a pair of words U_w^i, U_w^j and their respective contextual-lines U_l^i, U_l^j . Multimodal representations are obtained for each word and are then concatenated to form the input to the network $Z(U_w, U_l)$. The network is composed of two Dropout-Linear-ReLU blocks, followed by a Dropout-Linear block. Finally, we compute the affinity of the two projected multimodal embeddings using the affinity function σ as described in Section 3.

user-specified ones. Please refer to our accompanying video for a demonstration of our interactive system.

9 IMPLEMENTATION DETAILS

To learn the semantic affinities among words in an image, we use a multimodal encoder neural-network (see Figure 7 for a visualization of the network architecture). Throughout the evaluation of our method in the experiments described below, the method was run as follows: During train time, we employ the network as a Siamese encoder with shared weights for each pair of words in the image. To tune the network, we train it using artificial labels originating from our own generated auto-constraints ($y_c = 1$ for constraint $c \in E_{\text{must-link}}$, and similarly $y_c = 0$ for constraint $c \in E_{\text{cannot-link}}$) as detailed in section 6.2. For loss function, we employ cross-entropy loss over the affinity function σ , also described in the aforementioned section. In addition we perform clipping for gradients of magnitude larger than 5, to increase training robustness.

Our network architecture draws inspiration from [Xie et al. 2016] with slight pruning to the depth of the network, to ensure faster training. Specifically, let D represent the dimensionality of $Z(U_w, U_l)$. Thus the network dimensions are $D - 50 - 2000 - d$, where D is determined by the dimensionality of the style, content and geometry encoders, typically set to 512, 4096 and 4 respectively. In our work we set $d = 20$, which is low enough to avoid intricacies involved with clustering of high-dimensional data, yet high enough to contain information required for proper separation to clusters on typical documents.

For the initialization of the network, we follow the practice of [Xie et al. 2016] and draw random weights for a zero-mean normal distribution, with standard deviation of 0.01. For training, we freeze the embedding layers weights, and train the network for 100 epochs, with learning rate of $1e^{-4}$ and batch size of 32, using an Adam Optimizer [Kingma and Ba 2015]. For all our encoder blocks, we use a dropout of 0.2. Furthermore, to speed up the training on denser

Selection Method	Menus		Simple		Dense		Average	
	Items	Desc.	Items	Desc.	Items	Desc.	Items	Desc.
#words	31.8	118.9	20.8	66.7	16.9	394.3	21.7	193.3
#lines	13.8	26.2	10.8	19.1	4.6	48.7	9.7	31.3
#boxes	8.3	8.6	4.7	4.7	4.1	5.1	5.7	6.1
ours	2.0	0.5	0.5	0.3	0.4	0.3	1.0	0.3

Table 1. The user study results, comparing the number of post-optimization user edits to manual selection methods. We compare the number of user-scribble constraints needed using our approach against three baseline counting mechanisms, counting the number of words (#words), lines (#lines) and rectangular drag boxes (#boxes) needed to group the corresponding categories items and item descriptions (Desc.) correctly. Lower is better.

documents, we allow a maximum of 1000 must-link constraints, randomly-sampling the constraints if needed. Doing so allows us to cap the training runtime at up to one minute on a machine equipped with a single Tesla V100-SXM2 GPU.

Our method is implemented in Pytorch, and can be further optimized. Our experiments show that the entire pipeline converges within 35 seconds on average documents of 200 words, when allowing refinement to run for 60 epochs. Most of the pipeline time is spent on embeddings optimization. In the interactive mode, where the user marks additional constraints to improve the given clusters, we only re-run the Siamese network part of the pipeline, for a smaller amount of epochs. The refinement phase is tunable for a speed-accuracy tradeoff, and each optimization epoch takes about 0.5 seconds. For a common document of 300 words, a refinement of 10 epochs, which we found was sufficient for convergence, would take up to 5 seconds. We include a detailed latency report in our supplementary material.

10 RESULTS AND EVALUATION

We evaluated our technique on a new public dataset that we provide, of 50 highly varying images that have complicated layouts and span a wide range of documents, including menus, schedules, brochures and maps. To quantitatively evaluate the quality of our propagation results, we conducted a user study. Additionally, we performed a comparison between our approach and previous works in document-image analysis, clarifying the gap between the objectives of these works and our objective. We also performed a qualitative ablation study, demonstrating the importance of the multimodal approach and the optimization scheme. Finally, we demonstrate generalization capabilities onto nearby domains. In what follows, we elaborate on each of these experiments. We then conclude by discussing limitations of our presented approach.

10.1 User Study

We conducted a user study to quantitatively evaluate the quality and efficiency of our edit propagation system. As a semantic grouping is not entirely a well-defined task in the general case, we defined known categories and asked users to mark manual constraints and re-run the optimization until these known categories are grouped correctly. We quantitatively compare the number of manual constraints defined by the user against manual approaches, counting



Fig. 8. **User study image samples.** Users were presented with images capturing menus (top row), simple documents (middle row) or dense documents (bottom row). They were asked to manually mark constraints until the predefined category, items or item descriptions (paragraph titles and paragraphs in the case of dense documents), were grouped correctly. Above we illustrate a few samples with our automatically obtained grouping, which were later refined by the users. Please refer to the supplementary material for the full image sets used in the study.

the number of selections users would need to mark without our framework.

We collected three sets of images capturing (i) menus, (ii) simple and (iii) dense document-images, where each set contains 10 images in total. We defined two categories of interest in each set: items and item descriptions. In the case of menus, these are the items offered at the restaurant, and the corresponding item descriptions. Simple document-images are relatively sparse and for the most part contain these two categories only. Dense document-images capture mostly academic manuscripts or magazines, and in this case, the items are defined to be the paragraph titles and the item descriptions are defined to be the paragraphs of text. See Figure 8 for a few samples presented in our study, along with our corresponding automatic grouping result. For the full image sets used in the study, please refer to the supplementary material.

The participants were first presented with instructions on how to select must-link and cannot-link constraints in our interactive system. Thirty users in the age range 26-50 participated in the study (with a 1.14 male to female ratio). Each participant was provided

with 10 images belonging to one specific set and asked to evaluate the grouping of only one of the two categories. They were asked to add constraints and re-run the optimization until the grouping of that category was perfect. In other words, the users marked constraints until all the items/item descriptions were selected in a single group and no other words were included in that group.

We evaluated the quality of our automatically obtained result and of our interactive system by counting the number of user scribbles selected as constraints. By definition, a must-link constraint requires at least one scribble and specifies a group of words which should be clustered together, and a cannot-link constraint requires at least two scribbles and specifies two groups of words which should not be clustered together. To demonstrate that our system provides a more efficient way to propagate edit operations over simple counting mechanisms, we compared the number of manual constraints needed to three baselines that count the number of selections needed to group the words in the category. The most naive baseline counts the number of words in the category. The second baseline counts

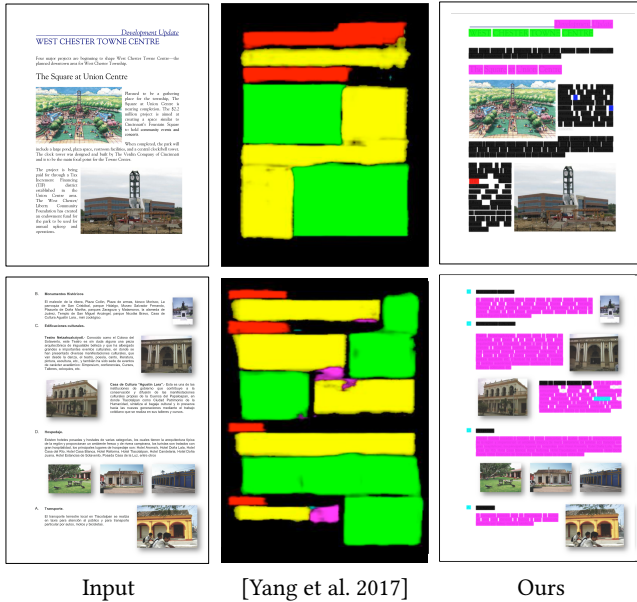


Fig. 9. **Comparison to previous work.** Previous work segment a document image into labelled regions (color legend: **figure**, **section heading**, **caption**, and **paragraph**). While a general document structure can be inferred from these predefined classes, they do not allow for recovering the semantic affinities among words in the image. Semantically and visually unique regions may be merged into one labeled region (for example, the names and job titles in the top row). Our result is illustrated on the right, where the semantic groups are marked in unique colors.

the number of horizontal lines in the category. Lastly, the third baseline counts the number of rectangular drag boxes needed to fully mark the category of interest; this baseline is proposed as editing softwares could optionally offer this functionality.

Table 1 summarizes the results of our user study. For each set, we average over the results, where for each image we use the maximum number of words and scribbles needed to correctly group the predefined category. For example, on average, 0.5 user-scribbles are needed to fix the grouping of the menu item descriptions, while 8.6 rectangular drag boxes would be needed to achieve this grouping manually from scratch (which amount to a selection of 118.9 words on average).

As the table illustrates, on average less than one scribble was needed to fix the initial grouping result. In contrast, more than five rectangular drag boxes are needed to mark the words in the predefined category, thus suggesting that our system can allow for a more efficient solution in selecting a category of words in a document-image. In the supplementary material, we provide all the images in the user-study along with the full comparison.

10.2 Comparison to previous work on document-images

Previous works analyzing document-images assume a supervised setting and aim at segmenting the document image into a fixed set of labeled regions (e.g., section heading or paragraph). To illustrate the gap to our style- and content- aware edit propagation technique,

in Figure 9, we compare our results to the segmentation results obtained by Yang et al. [2017].

As the figure illustrates, a segmentation technique which learns a predefined set of labels cannot allow for a fine-partitioning of the words within the image. See, for example, the names and job titles on the top row of Figure 9. They are both marked as “caption”, although semantically and visually these regions are not the same.

10.3 Qualitative Ablation Results

To demonstrate the importance of the various stages in our pipeline, we provide qualitative ablation results and demonstrate that removing components from our solution decreases its quality substantially for various use cases. To further assess the results, please refer to the supplementary materials where we provide interactive ablation results for dozens of document-images, spanning a wide range of categories as well as results obtained in a supervised setting, training on multiple documents.

Affinity space optimization. We illustrate the importance of the optimization stage in our algorithm, which includes the training process of the Siamese Neural Network. To assess the quality of the grouping results without the optimization stage, we perform the following modifications to our pipeline: we use Kernel-PCA to project the high-dimensional representation to a lower dimensional space (setting the output dimensionality to d_{out}). To cluster the projected representations, we use an edge-weighted graph as described in Section 7. However, as the neural net is unavailable, we employ a different predicate for the edge weights, using normalized Euclidean distance between pairs of words. For each pair of contextual lines, all pairwise distances of the enclosed words are averaged to yield the final affinity weight.

In Figures 2, 3 and 4 we visualize the non-learned affinity space. As the figures illustrate, unlike the learned affinity space, the non-learned affinity space is not tightly clustered. As the examples in the supplementary material illustrate, the clustering distance threshold for this case is unstable, and the quality is significantly lower compared to our constraint-based affinity learning approach.

Multimodal representations. Both the space of word representations in our work, as well as the constraints we employ in order to map this space into clusters, rely on a multitude of embedding types, namely: style, content and geometry. We recognize that for some document domains, specific embedding types may be more useful than others, and therefore demonstrate some use cases showing the effect of removing the aforementioned information from our representations and constraints. Not surprisingly, the visual style seems to be the most effective cue, and in some cases, a visual analysis is sufficient in correctly grouping the words in the document-image. In Figure 10, we demonstrate results obtained using only visual style, style and content, style and geometry, and our full multimodal configuration.

In general, we argue that content embeddings enable our algorithm to differentiate between clusters sharing similar style traits, and yet have separate distinctive semantic properties. See, for example, the prices on the top of Figure 10, which is grouped together with the item names when the content information is missing. We also show that geometric attributes (size and location of words) are

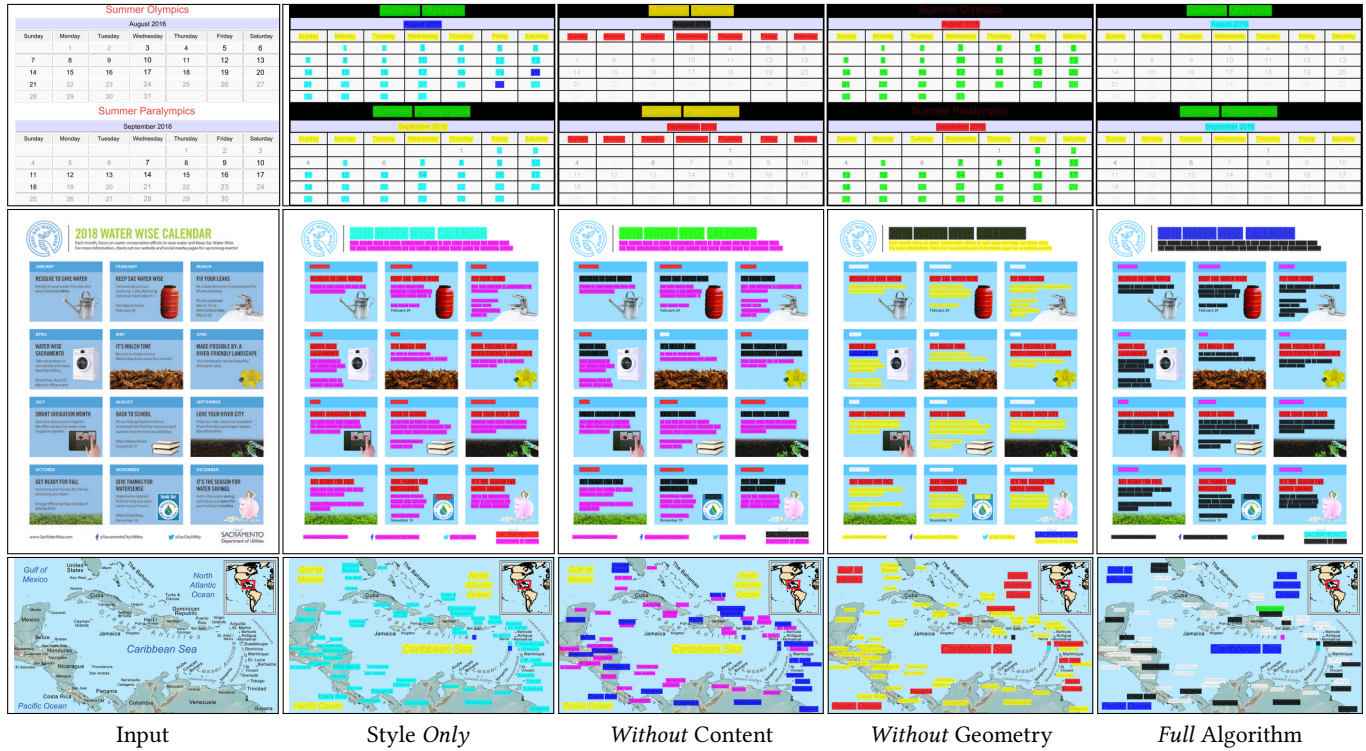


Fig. 10. Ablation analysis of our multimodal approach. We illustrate our grouping result with various multimodal configurations: only style (second to left), style and geometry (center), style and content (second to right), and our full multimodal configuration (left). Please refer to the supplementary materials for many more examples. Original images due to (top to bottom): © Felipe Menegaz, © City of SACRAMENTO, © Karl Musser.

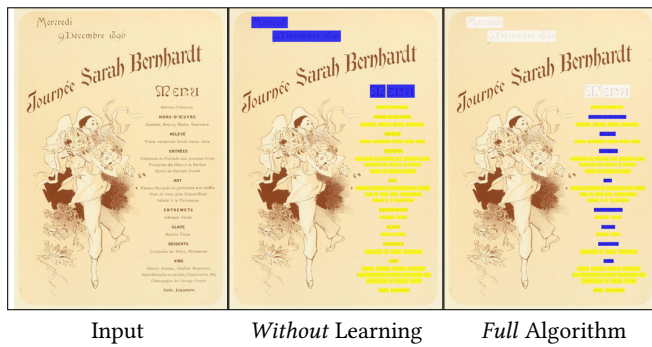


Fig. 11. Ablation analysis of our constraint-based affinity learning approach. We illustrate our grouping result with and without our optimization scheme. As the figure illustrates, without our optimization scheme only some of the words are grouped correctly. Please refer to the supplementary materials for many more examples. Original image © Double-M, Menu de la journée Sarah Bernhardt, le 9 décembre 1896.

useful to complement the visual description, in particular for the scenario where titles, headers and footers should be separated from other visually akin document elements harboring notably different functions. See, also, the map on the bottom of 10, where the configuration without geometry yields a grouping where the seas and some



Fig. 12. Our presented technique is also applicable for images captured in the wild, which contain only a small set of textual elements. Image courtesy Ron Shawley.

of the countries and cities are grouped together. In this example, our full configuration best separates the seas, countries and cities into distinct clusters.



Fig. 13. Learning affinities on scanned documents, which introduce various visual nuisances, as demonstrated above.

10.4 Generalization Capabilities

Next, we show results on more input types, without finetuning any parameters mentioned above, to demonstrate the generalization capabilities of our approach.

We examine our method on images *in the wild* that contain text (see Figure 12). While our propagation approach can more significantly boost performance in images that contain dozens of words, the editing operations can be performed on these images as well. It is important to note that, as our focus is on document-images, our solution is restricted for a 2D planar scenario. This implies, for instance, that our method will not cluster together text elements on two billboards at different depths in an image.

We also demonstrate results on scanned documents, that contain various artifacts, including blur, distortions, etc. (see Figure 13). These types of images are not only visually challenging, but also semantically, as the transcription is often erroneous. Nonetheless, our method is able to detect most of the unique clusters.

Furthermore, while our work focuses mostly with input images, containing rasterized documents, in the supplementary material we also demonstrate results of our algorithm on PDF documents, due to the proximity of this domain. The space of typical PDF documents can be roughly classified to documents with embedded images, which behave in a similar way to the document-images we process (text localization and transcription is not available in the input), as is usually the case with scanned documents. The other common group is PDF documents containing text elements. The latter renders the OCR step of our algorithm unnecessary, as the text information can be extracted directly from the input. Although the representation of basic units may be further enriched with meta-data excavated from the digital document, meaningful clusters must still be inferred by sophisticated means, which in turn makes the remainder of our pipeline necessary.



Fig. 14. **Contextual-line related limitations.** Our technique combines textual entities into the same contextual-line if the horizontal spacing between these entities is sufficiently small. However, as illustrated here, small horizontal space is not always a good indication of similar context.

10.5 Limitations

As a first step, our approach extracts the content and geometry of words using an off-the-shelf OCR solution. Thus, we are bounded by the accuracy of the OCR solution: errors from the OCR extraction phase are not fixed in later phases. OCR-related errors are evident in most figures, e.g., in Figure 12. While our algorithm is robust to these errors in most cases, in some cases, entire clusters are missed. For instance, as demonstrated in Figure 11, our OCR engine fails at recognizing curved text. However, as available OCR solutions scale up to these more challenging scenarios, they will immediately be handled by the rest of our pipeline.

To augment the word affinities with a contextual notion, we defined contextual-lines in the image (Section 4). Throughout our analysis, the contextual-lines serve as a basic building block, which we leverage multiple times. As we demonstrate, the contextual-lines allow for strengthening the initial multimodal representation. Furthermore, we use these lines to extract reliable pairwise connections from words within them in our optimization scheme, and ultimately propagate edits by grouping them.

Clearly, mistakes in the contextual-lines will lead to significant mistakes in the propagation result, which can only be corrected by user intervention. While our contextual-lines are defined conservatively and we deliberately avoid using any pretrained features in their selection, such mistakes are unavoidable. In Figure 14 we highlight an example, where the contextual-lines yield an undesirable grouping result as it merges two distinct regions.

Another notable limitation of our approach is that we analyze only the textual regions in the images, but in fact, a lot of documents contain regions of interest such as arrows, image sketches, or nested natural images. These may also assist in learning the affinities between the textual elements, and can even be considered as basic elements on their own right.

11 APPLICATIONS

In this section, we demonstrate the usefulness of our approach, presenting several novel text editing applications based on our grouping technique. The edit operations are propagated to textual elements all

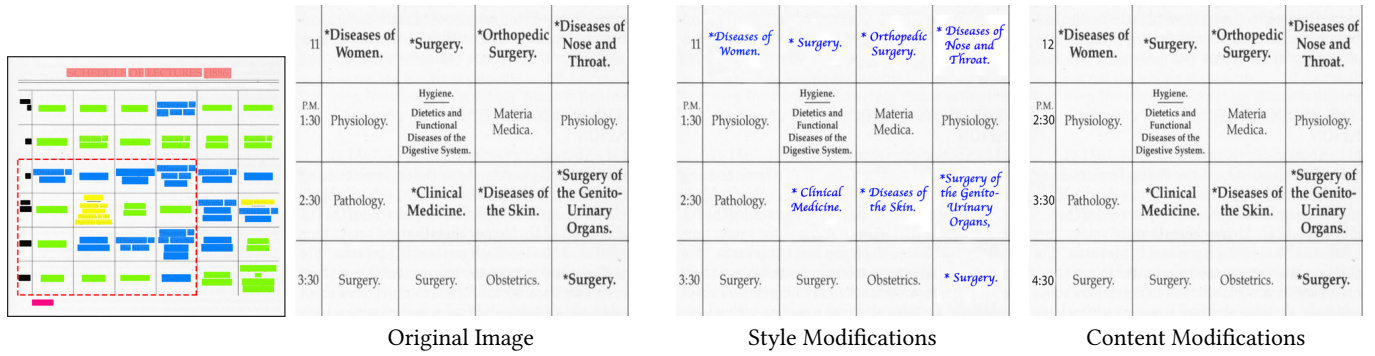


Fig. 15. **Style and Content Modifications.** We manipulate the style and the content of our global textual elements (colored in unique colors on the left). Style manipulations include modifications to font characteristics and font color (second image to the right), and content manipulations include mathematical operations. On the rightmost image, we modify the schedule by adding +1 to all time entities; note the left column of this image.

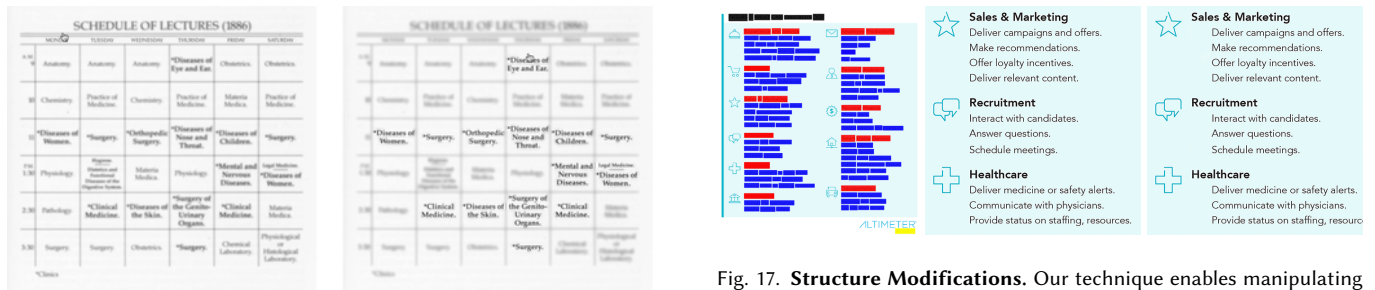


Fig. 16. **Emphasizing textual elements in the image.** Our technique enables propagating edits that emphasize textual elements of a certain type. For the extracted input image and the grouping result illustrated in Figure 15, the user can click a single word to emphasize a particular category of textual elements within the image.

across the image, thus significantly speeding-up the editing process. As previously discussed, editing textual content in a document-image can be a tedious task, especially if the amount of text entities is large, as the editing operations are repetitive in many cases. Below we illustrate examples of such potentially repetitive tasks. Our examples span style-based, content-based and geometry-based editing operations. Please refer to the accompanying video to view live editing examples.

Style-based Applications. Style-manipulation in images is a well-studied problem, especially recently due to advances in style transfer techniques (e.g., [Gatys et al. 2016; Zhu et al. 2017]). Within the context of local editing, some previous works focus on modifying the style of a region which captures a specific class, for example, a person [Shen et al. 2016].

We are interested in modifying the style of all textual elements of a given type. We demonstrate two different style manipulation modes: emphasizing regions of interest and manipulating stylistic parameters, such as font type or color.

In Figures 1 and 16, we illustrate two filtering operations that can be used to emphasize selected groups within a document-image.

Fig. 17. **Structure Modifications.** Our technique enables manipulating the structure of global elements. Above, we modify the horizontal location of the group that is colored in blue (on the leftmost figure) by indenting the text within this textual element. Image courtesy: Altimeter @ Prophet.

We use standard image filters, including sharpness, contrast and brightness to create a highlighting effect on the selected group.

To manipulate the stylistic parameters of the textual elements, we first need a mechanism to delete content within an image. For this purpose, we use a publicly available implementation of a standard image inpainting technique [Liu et al. 2018] to delete content within a given bounding box region. To keep the font family parameter fixed, we use the full classifier model described in Section 11 to select the best matching font for editing. In Figure 15, we illustrate manipulation results of the font parameters (second image to the right). This tool can also be used to emphasize (or de-emphasize) regions of interest.

Content-based Applications. Our technique can also facilitate propagating manipulations which are content-based. Indeed, our approach allows for fast propagation of semantic edits. In Figure 15, we illustrate the benefit of a semantic tool of this sort. As demonstrated in the figure, using our tool, one can easily and quickly apply direct mathematical operations to elements that represent numbers or dates.

Geometry-based Applications. Modifying the relative location and ordering of similarly looking text entities is a common text editing procedure in images. Figure 17 illustrates a typical use-case where the ability to seamlessly modify the document structure is useful.

Interactive Document-images. Document-images may contain excessive information, that may disturb the viewer’s focus. To reduce the visual load, we can use the mechanism previously described to delete certain content in the image, and bring it back interactively as the user hovers the mouse over a nearby textual region. This allows for a dynamic image, where the user can digest the content in a gradual manner, unlike a still image where the content appears all at once. See the accompanying video for a demonstration of an interactive document-image which can be quickly generated using our edit propagation technique.

12 CONCLUSIONS AND FUTURE WORK

We have presented an unsupervised method to learn affinities between words in a document-image, where the affinity reflects not only closeness in visual appearance, but also in the semantics of the underlying text. We optimized a multimodal affinity space by leveraging reliable pairwise connections in the data. Our pairs-based approach allows for the integration of additional supervised pairs which further enhances the affinity space. Technically, to learn an appropriate affinity using the pairwise connections, we represented the textual elements in the image in a multimodal manner that captures the style, content, and geometry of each word; and then optimized our affinity space with the help of a Siamese network, which embeds our multimodal word representation to a latent low-dimensional affinity space.

In a sense, our technique of grouping via unsupervised affinity learning can be seen as a way to *categorize* the textual elements in the image into several groups, or categories, that are learned in an unsupervised manner. This diverges significantly from most of the previous works on document analysis that usually partition the documents into categories labeled in advance, such as *title*, *paragraph title*, *paragraph*, and *caption*. The fact that our categories are learned in an unsupervised manner is essential to deal with various types of documents without prior knowledge on the document type and characteristics, and indeed, we show that our method performs well on many document types, including dense text documents, menus, calendars, maps, and brochures. The unsupervised grouping is shown to be useful in accelerating edit propagation, but in fact, it might serve as a new, generic way to represent and perceive documents of any type in a way that is similar to the human perception, and useful for document understanding applications.

In the future, we would like to further explore the relations and hierarchy between grouped textual elements in the image, tackling the problem of reconstructing text layout and re-flowing text from an input image. Another interesting avenue for future research is a multimodal image retrieval methodology, used to obtain document-images with similar style and content.

One application where our approach might be particularly useful is in digitization of documents with complex layouts. Digitization is the process of converting “real-world” information into a reliable computer-readable format. Substantial efforts have been dedicated to digitization of dense documents like books [Coyle 2006] and newspapers or journals [Clausner et al. 2017]. However, we are not aware of any generic digitization tool that can extract the textual content from *any* document while preserving the information

encapsulated in the structure of the document. Such a tool would need to understand high level relations between entities that are not necessarily co-located, and our embedding and grouping techniques might readily serve as a useful building block for tasks of this type.

REFERENCES

- Aishwarya Agrawal, Dhruv Batra, Devi Parikh, and Aniruddha Kembhavi. 2018. Don’t Just Assume; Look and Answer: Overcoming Priors for Visual Question Answering. In *IEEE Conference on Computer Vision and Pattern Recognition (CVPR)*.
- Alan Akbik, Duncan Blythe, and Roland Vollgraf. 2018. Contextual String Embeddings for Sequence Labeling. In *COLING 2018, 27th International Conference on Computational Linguistics*. 1638–1649.
- Teruo Akiyama and Norihiro Hagita. 1990. Automated entry system for printed documents. *Pattern Recognition* 23 (1990), 1141–1154.
- Xiaobo An and Fabio Pellacini. 2008. AppProp: all-pairs appearance-space edit propagation. In *ACM Transactions on Graphics (TOG)*, Vol. 27. ACM, 40.
- Stanislaw Antol, Aishwarya Agrawal, Jiasen Lu, Margaret Mitchell, Dhruv Batra, C. Lawrence Zitnick, and Devi Parikh. 2015. VQA: Visual Question Answering. In *International Conference on Computer Vision (ICCV)*.
- Henry S. Baird, Horst Bunke, and Kazuhiko Yamamoto. 1992. Structured Document Image Analysis. In *Springer Berlin Heidelberg*.
- Connelly Barnes, Eli Shechtman, Adam Finkelstein, and Dan B Goldman. 2009. Patch-Match: A randomized correspondence algorithm for structural image editing. *ACM Transactions on Graphics (TOG)* 28, 3 (2009), 24.
- Thomas M. Breuel. 2002. Two Geometric Algorithms for Layout Analysis. In *Document Analysis Systems V*, Daniel Lopresti, Jianying Hu, and Ramanujan Kashi (Eds.). Springer Berlin Heidelberg, 188–199.
- Thomas M. Breuel. 2003. High Performance Document Layout Analysis. In *Proceedings of the Symposium on Document Image Understanding Technology*.
- Zoya Bylinskii, Sami Alsheikh, Spandan Madan, Adria Recasens, Kimberli Zhong, Hanspeter Pfister, Fredo Durand, and Aude Oliva. 2017. Understanding infographics through textual and visual tag prediction. In *arXiv preprint arXiv:1709.09215*. <https://arxiv.org/pdf/1709.09215>
- Xiaowu Chen, Dongqing Zou, Qingping Zhao, and Ping Tan. 2012. Manifold preserving edit propagation. *ACM Transactions on Graphics (TOG)* 31, 6 (2012), 132.
- Zhuting Chen, Yun Wang, Qianwen Wang, Yong Wang, and Huamin Qu. 2020. Towards Automated Infographic Design: Deep Learning-based Auto-Extraction of Extensible Timeline. *IEEE Trans. Vis. Comput. Graph.* 26, 1 (2020), 917–926.
- C. Clausner, A. Antonacopoulos, and S. Pletschacher. 2017. ICDAR2017 Competition on Recognition of Documents with Complex Layouts - RDCL2017, Vol. 01. 1404–1410.
- Karen Coyle. 2006. Mass Digitization of Books. *The Journal of Academic Librarianship* 32, 6 (2006), 641 – 645.
- Kamran Ghasedi Dizaji, Amirhossein Herandi, Cheng Deng, Weidong Cai, and Heng Huang. 2017. Deep clustering via joint convolutional autoencoder embedding and relative entropy minimization. In *2017 IEEE International Conference on Computer Vision (ICCV)*. IEEE, 5747–5756.
- J. Donahue, L. A. Hendricks, M. Rohrbach, S. Venugopalan, S. Guadarrama, K. Saenko, and T. Darrell. 2017. Long-Term Recurrent Convolutional Networks for Visual Recognition and Description. *IEEE Transactions on Pattern Analysis and Machine Intelligence* 39, 4 (2017), 677–691.
- Zeev Farbman, Raanan Fattal, and Dani Lischinski. 2010. Diffusion maps for edge-aware image editing. In *ACM Transactions on Graphics (TOG)*, Vol. 29. ACM, 145.
- Alireza Fathi, Zbigniew Wojna, Vivek Rathod, Peng Wang, Hyun Oh Song, Sergio Guadarrama, and Kevin P. Murphy. 2017. Semantic Instance Segmentation via Deep Metric Learning. *CoRR* abs/1703.10277 (2017).
- Sharon Fogel, Hadar Averbuch-Elor, Jacov Goldberger, and Daniel Cohen-Or. 2018. Clustering-driven Deep Embedding with Pairwise Constraints. *IEEE Computer Graphics and Applications* (2018).
- Elena Garces, Aseem Agarwala, Diego Gutierrez, and Aaron Hertzmann. 2014. A Similarity Measure for Illustration Style. *ACM Transactions on Graphics (TOG)* 33, 4 (2014), 93:1–93:9.
- Leon A Gatys, Alexander S Ecker, and Matthias Bethge. 2016. Image style transfer using convolutional neural networks. In *Proceedings of the IEEE Conference on Computer Vision and Pattern Recognition*. 2414–2423.
- Ian Goodfellow, Jean Pouget-Abadie, Mehdi Mirza, Bing Xu, David Warde-Farley, Sherjil Ozair, Aaron Courville, and Yoshua Bengio. 2014. Generative adversarial nets. In *Advances in neural information processing systems*. 2672–2680.
- Yash Goyal, Tejas Khot, Aishwarya Agrawal, Douglas Summers-Stay, Dhruv Batra, and Devi Parikh. 2018. Making the V in VQA Matter: Elevating the Role of Image Understanding in Visual Question Answering. *International Journal of Computer Vision* (2018).
- Kaiming He, Xiangyu Zhang, Shaoqing Ren, and Jian Sun. 2016. Deep residual learning for image recognition. In *Proceedings of the IEEE conference on computer vision and pattern recognition*. 770–778.

- Max Jaderberg, Karen Simonyan, Andrea Vedaldi, and Andrew Zisserman. 2016. Reading Text in the Wild with Convolutional Neural Networks. *Int. J. Comput. Vision* 116, 1 (2016), 1–20.
- A. Karpathy and L. Fei-Fei. 2017. Deep Visual-Semantic Alignments for Generating Image Descriptions. *IEEE Transactions on Pattern Analysis and Machine Intelligence* 39, 4 (2017), 664–676.
- Rangachar Kasturi, Lawrence O’Gorman, and Venu Govindaraju. 2002. Document image analysis: A primer. *Sadhana* 27, 1 (2002), 3–22.
- Aniruddha Kembhavi, Mike Salvato, Eric Kolve, Minjoon Seo, Hannaneh Hajishirzi, and Ali Farhadi. 2016. A Diagram is Worth a Dozen Images. In *European Conference on Computer Vision (ECCV)*, Bastian Leibe, Jiri Matas, Nicu Sebe, and Max Welling (Eds.), 235–251.
- Diederik P. Kingma and Jimmy Ba. 2015. Adam: A Method for Stochastic Optimization. *CoRR abs/1412.6980* (2015).
- Yuanzhen Li, Edward Adelson, and Aseem Agarwala. 2008. ScribbleBoost: Adding Classification to Edge-Aware Interpolation of Local Image and Video Adjustments. In *Computer Graphics Forum*, Vol. 27. Wiley Online Library, 1255–1264.
- Guilin Liu, Fitsum A Reda, Kevin J Shih, Ting-Chun Wang, Andrew Tao, and Bryan Catanzaro. 2018. Image inpainting for irregular holes using partial convolutions. *arXiv preprint arXiv:1804.07723* (2018).
- Min Lu, Chufeng Wang, Joel Lanir, Nanxuan Zhao, Hanspeter Pfister, Daniel Cohen-Or, and Hui Huang. 2020. Exploring Visual Information Flows in Infographics. In *Proceedings of the 2020 CHI Conference on Human Factors in Computing Systems (CHI)*, 1–12.
- Spandan Madan, Zoya Bylinskii, Matthew Tancik, Adrià Recasens, Kimberli Zhong, Sami Alsheikh, Hanspeter Pfister, Aude Oliva, and Fredo Durand. 2018. Synthetically Trained Icon Proposals for Parsing and Summarizing Infographics. In *arXiv preprint arXiv:1807.10441*. <https://arxiv.org/pdf/1807.10441>
- Simone Meyer, Victor Cornillère, Abdelaziz Djelouah, Christopher Schroers, and Markus H. Gross. 2018. Deep Video Color Propagation. In *British Machine Vision Conference, BMVC*, 128.
- Lawrence O’Gorman. 1993. The document spectrum for page layout analysis. *IEEE Transactions on Pattern Analysis and Machine Intelligence* 15, 11 (1993), 1162–1173.
- Patrick Pérez, Michel Gangnet, and Andrew Blake. 2003. Poisson image editing. *ACM Transactions on graphics (TOG)* 22, 3 (2003), 313–318.
- Jorge Poco and Jeffrey Heer. 2017. Reverse-Engineering Visualizations: Recovering Visual Encodings from Chart Images. *Computer Graphics Forum* 36, 3 (2017), 353–363.
- Eric Saund, David Fleet, Daniel Lerner, and James Mahoney. 2003. Perceptually-supported Image Editing of Text and Graphics. In *Proceedings of the 16th Annual ACM Symposium on User Interface Software and Technology*, 183–192.
- Sohil Atul Shah and Vladlen Koltun. 2018. Deep Continuous Clustering. *CoRR* (2018).
- Xiaoyong Shen, Aaron Hertzmann, Jiaya Jia, Sylvain Paris, Brian Price, Eli Shechtman, and Ian Sachs. 2016. Automatic portrait segmentation for image stylization. In *Computer Graphics Forum*, Vol. 35. Wiley Online Library, 93–102.
- Ray Smith. 2007. An overview of the Tesseract OCR engine. In *Ninth International Conference on Document Analysis and Recognition (ICDAR 2007)*, Vol. 2, 629–633.
- Junyuan Xie, Ross Girshick, and Ali Farhadi. 2016. Unsupervised deep embedding for clustering analysis. In *International conference on machine learning*, 478–487.
- Jun Xing, Hsiang-Ting Chen, and Li-Yi Wei. 2014. Autocomplete Painting Repetitions. *ACM Trans. Graph.* 33, 6 (2014), 172:1–172:11.
- Kun Xu, Yong Li, Tao Ju, Shi-Min Hu, and Tian-Qiang Liu. 2009. Efficient affinity-based edit propagation using kd tree. In *ACM Transactions on Graphics (TOG)*, Vol. 28. ACM, 118.
- Jianwei Yang, Devi Parikh, and Dhruv Batra. 2016. Joint unsupervised learning of deep representations and image clusters. In *Proceedings of the IEEE Conference on Computer Vision and Pattern Recognition*, 5147–5156.
- Xiao Yang, Ersin Yumer, Paul Asente, Mike Kraley, Daniel Kifer, and C Lee Giles. 2017. Learning to Extract Semantic Structure From Documents Using Multimodal Fully Convolutional Neural Networks. In *Proceedings of the IEEE Conference on Computer Vision and Pattern Recognition*, 5315–5324.
- Jun-Yan Zhu, Taesung Park, Phillip Isola, and Alexei A Efros. 2017. Unpaired Image-to-Image Translation using Cycle-Consistent Adversarial Networks. In *IEEE International Conference on Computer Vision*.